American Journal of Physics and Applications
2026, Vol. 14, No. 5, pp. 91–98
https://doi.org/10.11648/j.ajpa.20261405.12

Research Article

Characterization of Plasma in Laser-Induced Breakdown Spectroscopy Through Fe I Spectral Lines Electron Temperature, Electron Density, Debye Length, and Debye Number

Altaf Alsaid Mohamed Abdalgader*

Laser Institute, Sudan University of Science and Technology, Khartoum, Sudan

Abstract

Cement is a widely used hydraulic binder composed primarily of calcium, silicon, aluminum, and iron oxides. This present work examines the plasma characteristics of cement sample through the analysis of neutral iron (Fe I) emission lines recorded using, laser-induced breakdown spectroscopy (LIBS). A Q-switched Nd: YAG laser, was used for plasma generation operating at a wavelength of 266 nm, with a pulse duration of 8 ns and a repetition rate of 10 Hz. The laser pulse energy was varied from 10 to 32 mJ. Emission features from Several neutral and ionic species were identified in the cement plasma, Four Fe I spectral lines were then used to estimate the electron temperature and electron density from the spectroscopic measurements at different laser pulse energies, and 200 ns delay. The Debye length and Debye number were subsequently calculated from the obtained plasma parameters. The results showed that increasing the laser pulse energy enhanced the plasma emission intensity and affected the plasma parameters. The obtained results demonstrate the applicability of Fe I spectral lines for characterizing the plasma generated from cement using LIBS and provide insight into the fundamental plasma properties under different laser excitation energies.

Keywords

Cement, Laser Induced Breakdown Spectroscopy, Laser Energy, Plasma Temperature, Electron Density, Debye Length, Debye Number

1. Introduction

Laser-induced breakdown spectroscopy is a technique that enables the analysis of elements and the simultaneous detection of multiple elements [1]. Wide range of samples can be applied. [2], These include solids, gases, and liquids, as well as aerosols. The fundamental principle of the laser-induced breakdown spectroscopy technique is that a high-energy laser pulse interacts with a target, producing plasma [3-5].

When a focused laser pulse is directed onto the sample surface, a small amount of material is ablated [6] and converted into excited plasma this plasma contains atoms, ions, and electrons [7]. The emitted radiation from the plasma is collected and analyzed using a spectrometer [7]. Each element produces

*Correspondence: Altaf Alsaid Mohamed Abdalgader (altafelsied@gmail.com)

Received: 29 September 2026; **Accepted:** 4 November 2026; **Published:** 19 November 2026

Copyright: © The Author(s), 2026. Published by Science Publishing Group. This is an **Open Access** article, distributed under the terms of the Creative Commons Attribution 4.0 License (http://creativecommons.org/licenses/by/4.0/), which permits unrestricted use, distribution and reproduction in any medium, provided the original work is properly cited.

characteristic spectral lines that can be used for its identification and analysis [4, 8, 9]. Laser-induced breakdown spectroscopy has been employed in various fields due to its rapid analysis capability and the fact that it requires minimal sample preparation for both qualitative and quantitative analysis. [10, 11]. LIBS provide an effective method for both detecting and analyzing samples simultaneously. [8, 12, 13].

In addition to elemental identification and quantification, the emission spectra generated by LIBS can be used to study the physical properties of laser-generated plasma [14]. Spectral lines from selected atomic species can provide valuable information about the plasma conditions and can be used to determine important plasma parameters [15]. In particular, Fe I spectral lines can be employed for the characterization of the plasma generated from complex materials such as cement.

In this study, LIBS was employed to investigate the plasma generated from a cement sample using Fe I emission lines. The electron temperature and electron density were determined from the recorded emission spectra at different laser pulse energies. Subsequently, the Debye length and Debye number were calculated to further characterize the plasma and evaluate its plasma properties. The obtained results provide a spectroscopic characterization of the cement-induced plasma under different laser excitation conditions.

2. Materials and Methods

2.1. Sample Preparation

The sample was prepared by applying a compressive force of 12 tons to 3 g of cement for 2 minutes, resulting in discs with a diameter of 2 cm. using hydraulic pressure.

2.2. LIBS Experimental Setup

LIBS setup is shown in Figure 1. The main apparatus in LIBS is the Laser, laser is used to generated plasma on the sample surface. In this system a pulsed Nd: YAG laser (266 nm) is used. A Q switch is used to generate a pulsed laser. The laser beam incidents on the sample (which is on an X-Y translation stage [8, 16].

The same cement sample and experimental setup used in our previous study [1] were employed in the present investigation. The laser pulse energy was varied over the same range (10 – 32mJ) specifically 10, 15, 20, 25, 30, and 32 mJ, laser pulse duration was 8 ns, and the pulse repetition rate was 10 Hz. The plasma emission was collected and analyzed using an Ocean Optics LIBS 2000+ spectrometer equipped with a gated CCD detector containing 14,336 pixels. The plasma emission was observed at an angle of 90 ° with respect to the incident laser beam. A delay time of 200 ns was used for the acquisition of the plasma emission spectra. to maintain consistent experimental conditions. While the previous study focused on the relationship between laser pulse energy and emission intensity along with the determination of electron temperature and electron density, the present work specifically investigates selected neutral iron Fe I spectral lines. In addition, the Debye length and Debye number are evaluated to provide further insight into the plasma characteristics and its collective behavior.

The recorded spectra were analyzed and the observed spectral lines were identified using the NIST Atomic Spectra Database.

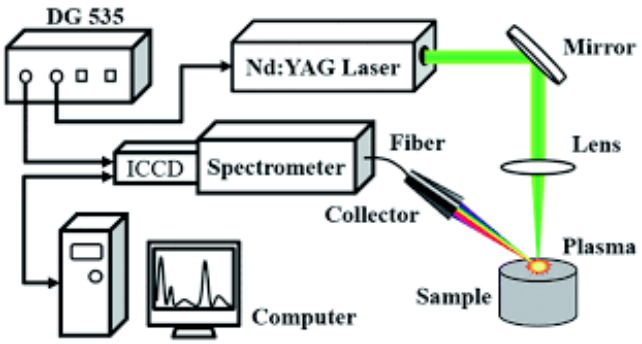


Figure 1. *Schematic diagram of the LIBS setup.*

3. Results and Discussions

3.1. LIBS Emission Spectra and Elemental Identification

Figure 2 Below presents the LIBS emission spectra recorded from the cement sample at different laser pulse energies of 10, 15, 20, 25, 30, and 32 mJ, using a delay time of 200 ns [1]. The recorded spectra revealed a number of clearly defined emission lines, corresponding to the various atomic and ionic species present in the cement plasma. These observed spectral lines were identified using the National Institute of Standards and Technology (NIST) Atomic Spectra Database.

The spectra generally show stronger emission at higher pulse energies. This behavior can be attributed to the greater amount of material ablated from the sample and the higher excitation and ionization of the plasma produced at higher laser energies. Consequently, the population of excited atoms and ions increases, leading to stronger characteristic emission lines.

The spectra reveal emission lines associated with several constituent elements of the cement sample, including Ca, Fe, Cr, Zr, Kr and other species. Both neutral atomic lines and ionic emission lines are observed, indicating the formation of energetic and highly excited plasma [8]. Among the detected species, Fe I emission lines were selected for further plasma characterization. These lines were subsequently used to determine the electron temperature and electron density, which were then employed to calculate the Debye length and Debye number.

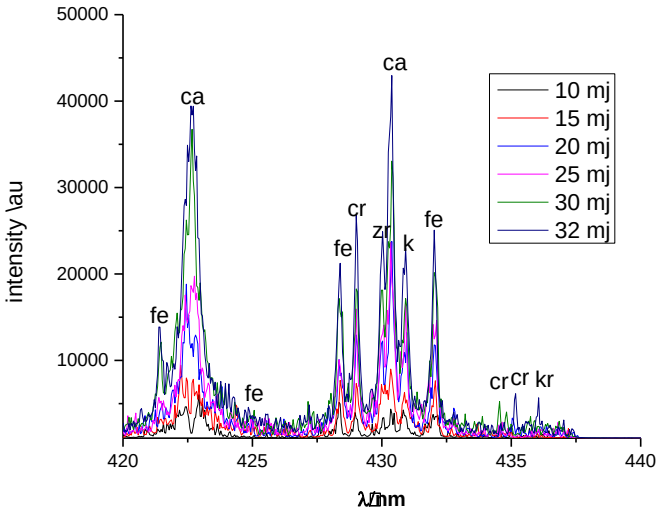


Figure 2. *LIBS spectra by different laser energy.*

3.2. Selected Fe1 Spectral Lines

Table 1. *Spectroscopic constant of Fe I.*

λ\nm	A_{ki}	g_i	g_k	E_i/ev	E_k/ev	ΔE/ev
421.61	$1.8*10^4$	9	9	0	2.9398	2.9398
425.078	$1.2*10^7$	7	7	1.5189	4.4732	2.9543
428.24	$1.21*10^7$	7	5	2.1759	5.0703	2.89
431.704	$5.2*10^5$	5	5	3.5965	6.4176	2.87

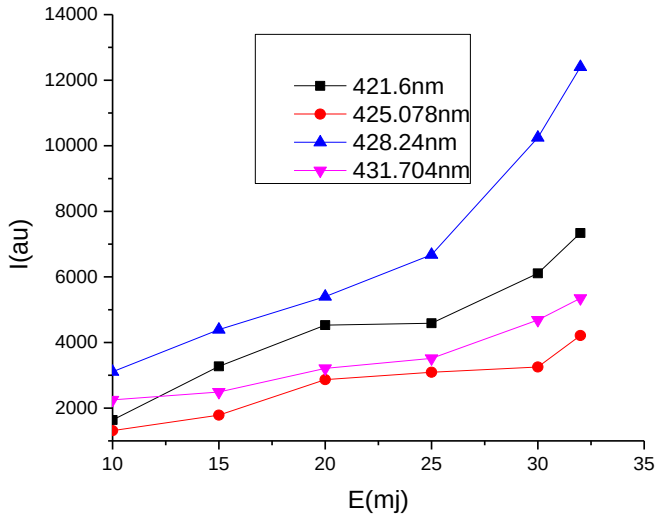


Figure 3. *Variation of Plasma intensity with laser pulse energy at Fe I spectral lines.*

3.3. Electron Temperature

Electron temperature was estimated from Fe I emission lines from 421.61 nm to 431.7nm by using equations (1 and 2) The line intensity relationship used in this calculation is given in equation (1) [16].

$$I = \frac{hcgAN}{4\pi\lambda U} e^{-E/kT} \quad (1)$$

In this equation, h denotes Planck's constant, c is the speed of light, λ is the transition wavelength, g is the statistical weight of upper state, E is the upper –level energy, U is the partition function, K is the Boltzmann constant and T is the electrons' temperature. taking the natural logarithm gives the form shown equation (2).

$$\ln\left(\frac{I\lambda}{Ag}\right) = \frac{-E}{KT} + \ln\left(\frac{hcN}{4\pi U}\right) \quad (2)$$

For a given species, the terms that do not depend on the upper –level energy are treated as constant. Accordingly a plot of Ln (Iλ/Ag) against E for several emission lines is expected to be linear its slope is used to determine the electron temperature.

For pulse energies of 10, 15, 20, 25, 30 and 32 mJ the calculated Electron temperature were 5606 K, 5873K, 6140K, 6173K, 6273K and 6342K Respectively.

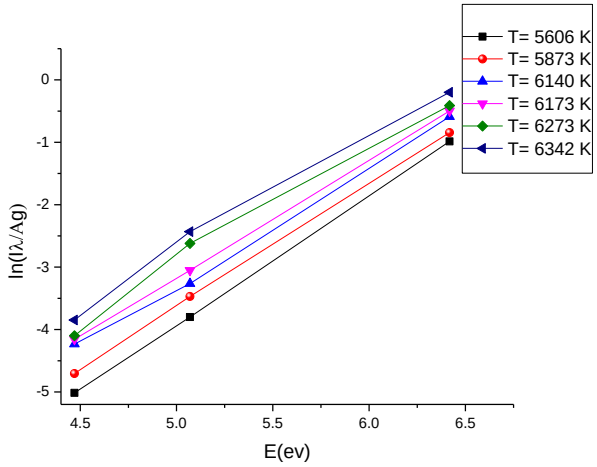


Figure 4. *Electron temperatures at different laser pulse energy.*

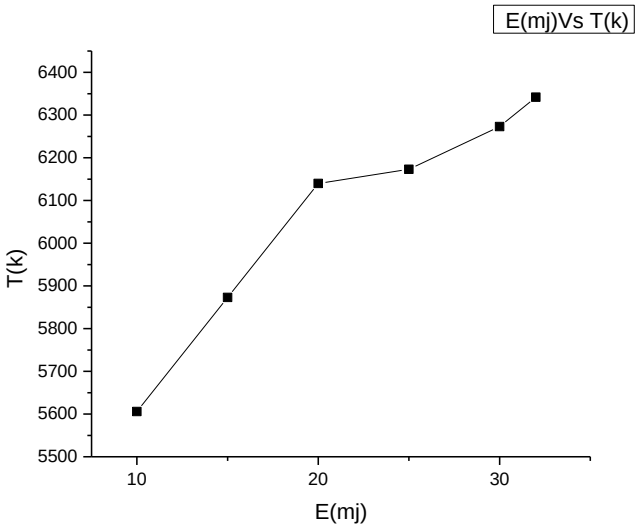


Figure 5. *Dependence of electron temperature on laser energy variation.*

The observed electron temperature increased with increased in laser pulse energy, increasing the laser pulse energy delivers more energy to the sample and the resulting plasma; consequently, heating, excitation, and ionization processes intensify, which may lead to a rise in electron temperature.

3.4. Electron Density

The electrons density at Fe I lines was calculated using equation below [17].

$$n_e = 1.6 * 10^{12} T_e^{1/2} \Delta E^3 \quad (3)$$

where n_e is electron density, T_e electron temperature (K), ΔE the largest observed transition energy (eV). the values were evaluated for pulse energies of (10, 15, 20, 25, 30 and 32 mJ, at 200ns delay time.

Table 2. *Electron temperatures and electron densities at different laser energies of Fe I lines:*

E\mj	T\k	n_e*$10^{16} cm^{-3}$			
		Fe Iat 421.61nm	Fe I at 425.078nm	Fe I at 428.24nm	Fe I at 431.704nm
10	5606	3	3.08	2.89	2.83
15	5873	3.1	3.2	2.96	2.9
20	6140	3.2	3.23	3.03	2.97
25	6173	3.3	3.24	3.046	2.97
30	6273	3.32	3.27	3.06	2.99
32	6342	3.37	3.29	3.08	3.01

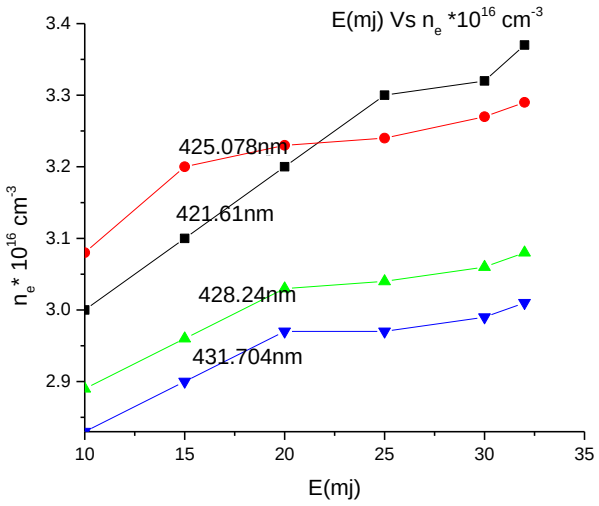


Figure 6. *Dependence electron density of laser pulse energy.*

An increase in electron density has been observed with increasing laser energy; this implies that higher laser energy leads to a greater amount of vaporized material and, consequently, enhanced ionization, resulting in a higher number of free electrons and, ultimately, increased electron density.

3.5. Debye Length

The Debye length characterizes the distance over which electric fields are screened by mobile charges in plasma [18]. Its value determined the electron temperature and electron density, using the relation given below.

$$\lambda_D = \sqrt{\frac{\varepsilon_0 k_B T_e}{n_e e^2}} \quad (4)$$

In this expression, ε_0 Permittivity of free space (8.854 * 10^{12} F/m), k_B Boltzmann's constant (1.38 * 10^{-23} J/K),T_e: Electron temperature (in Kelvin), n_e: Electron density cm^{-3}, e: Elementary charge (1.602 * 10^{-19} C) [19]. From the previous equation we obtained:

$$\lambda_D = 69\sqrt{\frac{T_e}{n_e}} \quad (5)$$

Thus we calculated Debye length for Fe I spectral lines (421.61 nm, 425.087nm, 428.24nm, 431.704nm) dependent on electron temperatures and electron densities. That obtained in table below:

Table 3. *Shows the relationship between plasma temperature, electron density, and Debye length for four Fe 1 spectral lines.*

T\k	n_e*$10^{16}cm^{-3}$				λ_D\nm			
	Fe I at 421.61nm	**Fe I at 425.078nm**	**Fe I at 428.24nm**	**Fe I at 431.704nm**	**Fe I at 421.61nm**	**Fe I at 425.078nm**	**Fe I at 428.24nm**	**Fe I at 431.704nm**
5606	3	3.08	2.89	2.83	29.8	29.5	30.4	30.8
5873	3.1	3.2	2.96	2.9	30.1	29.6	30.8	31.1
6140	3.2	3.23	3.03	2.97	30.3	30.1	31.1	31.4
6173	3.3	3.24	3.04	2.98	29.9	30.2	31.1	31.5
6273	3.32	3.27	3.06	2.99	30	30.3	31.3	31.7
6342	3.37	3.29	3.08	3.01	30	30.3	31.4	31.7

Based on the results shown in the table above, we observe that the Debye length depends simultaneously on both electron temperature and electron density. It was found that when electron temperature remains constant while electron density varies, the Debye length decreases as electron density increases. Conversely, the Debye length was observed to increase with rising electron temperature—even as electron density increased—indicating that the temperature effect is dominant in this instance. Notably, at a temperature of 6173 K and the 421.61 nm line, the Debye length decreases slightly, demonstrating that the increase in electron density drove this reduction. We can thus conclude that changes in the Debye length within plasma are not determined solely by temperature, but rather by the simultaneous variation in T_e and n_e.

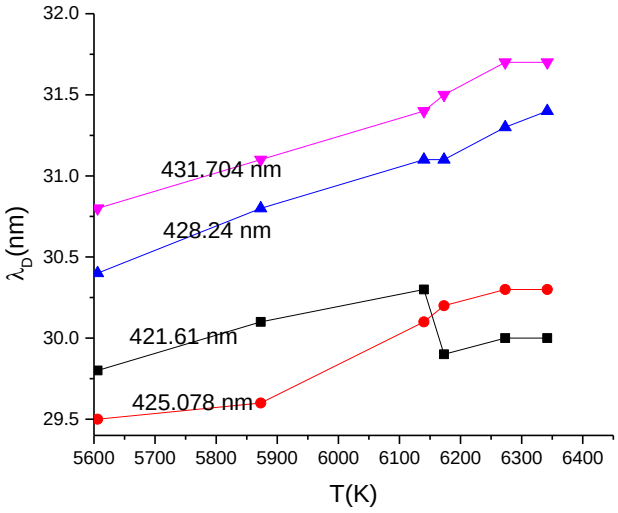


Figure 7. *Debye length variation by electrons temperature.*

3.6. Debye Number

Debye number N_D, represents the number of charged particles within Debye sphere [20]. it was calculated using equation 6:

$$N_D = \frac{4}{3}\pi n_e \lambda_D^3 \quad (6)$$

The calculated Debye numbers were obtained from the electron density, and Debye length values The result for each temperature and selected Fe I lines are presented in Table 4.

Table 4. Debye number at different electrons temperature and different electrons density.

T\k	N_D			
	Fe I at 421.61nm	Fe I at 425.078nm	Fe I at 428.24nm	Fe I at431.704nm
5606	3.34	3.29	3.4	3.44
5873	3.52	3.46	3.60	3.64
6140	3.70	3.69	3.81	3.84
6173	3.68	3.71	3.83	3.87
6273	3.75	3.78	3.91	3.96
6342	3.79	3.83	3.96	4.01

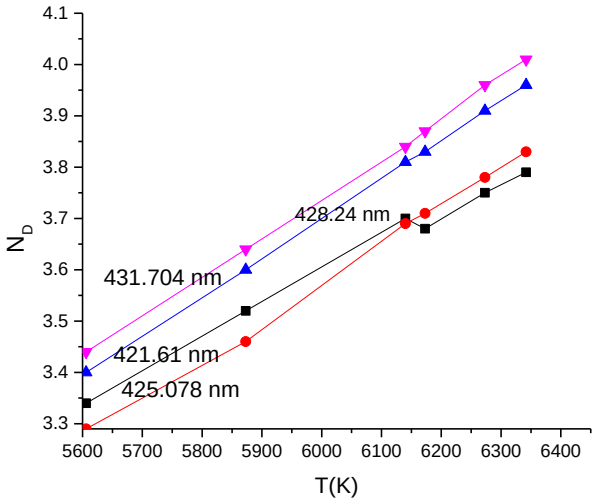


Figure 8. Debye number dependence on electron temperature.

From results we observed Debye number tend to increase with increasing electron temperature and calculated Debye number ranges from approximately 3.3 to 4.0 for the investigated Fe I lines. Since the plasma exhibits Debye shielding and collective behavior. However, the relatively low values of N_D indicate that the collective character is not very strong.

4. Conclusion

In this work, used Fe I emission lines to characterized laser – induced plasma produced from a cement sample. Across the investigated pulse energies, the estimated electron temperature ranged from 5606 to 6342 K, and the electron density was of the order of $10^{16} cm^{-3}$. The calculated Debye length was approximately 29.5–31.7 nm for the investigated spectral lines. The Debye number (N_D), varied from about 3.29 to 4.01. The results generally showed an increasing tendency of N_D, with increasing electron temperature. However, the relatively small values of N_D, indicate that only a few charged particles are contained within the Debye sphere, suggesting relatively weak collective behavior under the investigated plasma conditions. These results provide useful information for assessing the plasma characteristics and the applicability of Debye shielding concepts in Fe-based LIBS plasma.

Abbreviations

LIBS	Laser Induced Breakdwn Spectroscopy
Nd:YAG	Neodymium - doped Yttrium Aluminum Garnet
NIST	National Institute of Standards and Technology
CCD	Charge-Coupled Device
T_e	Electron Temperature
n_e	Electron Density
λ_D	Debye Length
N_D	Debye Number

Author Contributions

Altaf Alsaid Mohamed Abdalgader: Conceptualization,

Formal Analysis, Investigation, Methodology, Writing – original draft

Conflicts of Interest

The author declares no conflict of interest.

References

[1] Altaf A Mohamed, Abdelmoneim Awadelgied, Use laser induced breakdown spectroscopy in detection of heavy metals contents in Sudanese cement, International Journal of Physics and Applications (2022), https://doi.org/10.33545/26647575.2022.v4.i1a.42

[2] Qin et al. Proteome Science 2013, 11:12 http://www.proteomesci.com/content/11/1/12

[3] Sergio Musazzi, Umberto Perini, Laser-Induced Breakdown Spectroscopy. Theory and Applications, springer nature, 2014.

[4] Gondal, M. A., Hussain, T., Yamani, Z. H. et al. Determination of Toxic Metals in Petroleum, Cultivated Land and Ore Samples Using Laser-Induced Breakdown Spectroscopy. Bull Environ Contam Toxicol 78, 270–274 (2007). https://doi.org/10.1007/s00128-007-9141-7

[5] Gupta, A. K., Srivastava, Y., & Mishra, P. (EdsNovel Techniques for Food Quality Analysis and Safety: Fundamentals, Scope, Feasibility, and Challenges (1st ed.). CRC Press.). (2026). https://doi.org/10.1201/9781003482611

[6] R. S. Harmon& R. E. Russo, Laser-Induced Breakdown Spectroscopy, Treatise on Geochemistry (Second Edition), 2014, https://doi.org/10.1016/B978-0-08-095975-7.01417-0

[7] M. Capitelli, A. Casavola, G. Colonna & A. De Giacomo, Laser-induced plasma expansion: theoretical and experimental aspects, Spectrochimica Acta Part B: Atomic Spectroscopy, (2004), https://doi.org/10.1016/j.sab.2003.12.017

[8] Altaf Alsaid Mohamed Abdalgader, Abdelmoneim Awadelgied. Studying the Effect of Delay Time on Intensity of Laser Induced Breakdown Spectroscopy Technique Using Mas Cement Sample. World Journal of Applied Physics. Vol. 7, No. 1, 2022, pp. 11-15. https://doi.org/10.11648/j.wjap.20220701.12

[9] Hussain, T., Gondal, M. A., Yamani, Z. H. et al. Measurement of Nutrients In Green House Soil With Laser Induced Breakdown Spectroscopy. Environ Monit Assess 124, 131–139 (2007). https://doi.org/10.1007/s10661-006-9213-x

[10] Syed Kifayat Hussain Shah, Javed Iqbal, Pervaiz Ahmad, et al, Laser induced breakdown spectroscopy methods and applications: A comprehensive review, Radiation Physics and Chemistry, 2019, https://doi.org/10.1016/j.radphyschem.2019.108666

[11] Salih, Fatima H.; Mahdi, Shaimaa S.; and Ali, Alaa H. (2025) "Employment of Laser Induced Breakdown Spectroscopy to Determine Elements of Human Hair," *Baghdad Science Journal*: Vol. 22: Iss. 3, Article 20. https://doi.org/10.21123/bsj.2024.10388

[12] Marc N. Fiddler, Israel Begashaw, Matthew A. Mickens et al. Laser Spectroscopy for Atmospheric and Environmental Sensing. *Sensors* 2009, *9*, 10447-10512; https://doi.org/10.3390/s91210447

[13] Muhammad FAHAD, Sajad ALI, Yaseen IQBAL. Plasma diagnostics by optical emission spectroscopy on manganese ore in conjunction with XRD, XRF and SEM-EDS [J]. Plasma Science and Technology, 2019, 21(8): 85507-085507. https://doi.org/10.1088/2058-6272/ab1977 (2019), 8, 085507.

[14] Moros J& Laserna J. Laser-Induced Breakdown Spectroscopy (LIBS) of Organic Compounds: A Review. Applied Spectroscopy. 2019; 73(9): 963-1011. https://doi.org/10.1177/0003702819853252

[15] Baida M. Ahmed, Plasma Parameters Generated from Iron Spectral Lines byUsing LIBS Technique, IOP Conf. Ser.: Mater. Sci. Eng. 928 072096 (2020). https://doi.org/10.1088/1757-899X/928/7/072096

[16] T. Hussain *et al* Determination of plasma temperature and electron density of iron in iron slag samples using laser induced breakdown spectroscopy, 2016, *IOP Conf. Ser.: Mater. Sci. Eng.* 146 012017. https://doi.org/10.1088/1757-899X/146/1/012017

[17] Ashwin P. Rao, Mark Gragston, Anil K. Patnaik, et al, Measurement of electron density and temperature from laser-inducednitrogen plasma at elevated pressure (1–6 bar), Optics Express,(2019), Vol. 27, Issue 23, pp. 33779-33788. https://doi.org/10.1364/OE.27.033779

[18] Asokan Ajith, Mohanachandran Nair Sindhu Swapna, Humberto Cabrera and Sankaranarayana Iyer Sankararaman, Comprehensive Analysis of Copper Plasma: A Laser-Induced Breakdown Spectroscopic Approach. photonics, (2023), 10, 199.

[19] D. M. Goebel and I.Katz. fundamenatals of electric propulsion: Ion and Hall thrsters, 1st ed. hoboken, NJ, USA: John Wiley & Sons, 2008, https://doi.org/10.1002/9780470436448

[20] Gibbon, P. Introduction to Plasma Physics. In Proceedings of the 2014 CASCERN Accelerator School: Plasma Wake Acceleration, Geneva, Switzerland, 23–29 November 2014; pp. 51–65.